Development of Bortezomib-Loaded Nanoparticles for Locoregional Treatment of Hepatocellular Carcinoma

by

Yang Zhou

A thesis submitted to The Johns Hopkins University in conformity with the requirements for the degree of Master of Science

Baltimore, Maryland

May 2020

Abstract

Hepatocellular carcinoma (HCC) is the 6th most common cancer and the 4th leading cause of carcinoma-related death worldwide; yet there no curative chemotherapy strategy available for unresectable HCC. Bortezomib (BTZ) is a proteasome inhibitor that is FDA-approved for multiple myeloma and certain subtypes of chronic myelogenous leukemia; and in drug screening tests it shows promising potency in HCC cells. Systemic administration at required doses proves to be toxic in mice, however, repeated intra-tumoral injections results in tumor regression. The objective of this study is to develop a BTZ-loaded nanoparticle that can lower the systemic toxicity through local release of BTZ over several days. The BTZ-loaded nanoparticles were prepared by a facile assembly technique combining flash nanocomplexation (FNC) and flash nanoprecipitation (FNP), achieving high uniformity, stability, and adjustability by controlling the input parameters during preparation process. In the pilot *in vivo* study, the BTZ-loaded nanoparticles demonstrated local retention for more than 10 days in tumor tissue following intratumoral injection and exerted similar tumor-killing effect with same dose, yet less injection frequency as compared to free BTZ. The BTZ-loaded nanoparticles exhibited potential as a locoregional delivery system to provide a new therapeutic modality for future HCC treatment.

Primary Reader and Advisor: Hai-Quan Mao

Acknowledgments

I would like to thank Prof. Hai-Quan Mao, Prof. Florin Selaru, Dr. Ling Li, and my fellow lab mates Kuntao Chen, Gregory Howard, and Zhiyu He for their generous help and valuable advice that support me to finish this project. I would like to thank my parents, my advisor, everyone in our lab and my friends who have supported me all the way.

Contents

Abstract iii

Acknowledgments 3

1. Introduction 1

2. Materials and Methods 4

2.1 Device and materials 4

2.2 BTZ-loaded nanoparticle preparation 4

2.3 Characterizations 5

2.4 Storage stability study 6

2.5 In vitro release study 6

2.6 MTT Assay 7

2.7 In vivo retention study using *Cy 7.5* labelled nanoparticles 7

2.8 In vivo therapeutic effect of BTZ-loaded nanoparticles 8

3. Results and Discussion 9

3.1 Formulation screening and characterization of the BTZ-loaded nanoparticles 9

3.2 In vitro release study of BTZ-loaded nanoparticles 12

3.3 In vitro efficacy of BTZ-loaded nanoparticles 14

3.4 In vivo retention effect in tumor tissue following intratumoral injection of BTZ-loaded nanoparticles 15

3.5 In vivo tumor-inhibition effect of BTZ-loaded nanoparticles in patient derived xenograft (PDX) model..... 16

4. Conclusion 19

5. References..... 20

List of Tables

Table 1. Characteristics of freshly prepared vs. lyophilized-and-reconstituted BTZ-loaded nanoparticles..... 12

List of Figures

Figure 1. Schematic illustration of the sequential FNC /FNP method utilized in the BTZ-loaded nanoparticle preparation process. 9

Figure 2. Formulation screening of the sequential FNC/FNP process 10

Figure 3. Characterization of BTZ-loaded nanoparticles 11

Figure 4. In vitro release study of different BTZ nano-formulations 12

Figure 5. In vitro bioactivity evaluation of BTZ-loaded nanoparticles. 14

Figure 6. Biodistribution of the fluorescent dye-labeled nanoparticles after intra-tumoral injection. 15

Figure 7. In vivo therapeutic outcomes of BTZ-loaded nanoparticles. 17

Chapter 1

Background and Significance

In 2019, the incidence of liver cancer is estimated to be about 42,000 in United States and 840,000 worldwide, posing a great threat to human health. Among all the liver cancer patients, hepatocellular carcinoma (HCC) accounts for 80–85% of all cases of primary liver cancers[1]. However, there is currently no curative chemotherapy strategy on the market for unresectable advanced cancer. Some experts have even hypothesized that HCC is "not druggable"[2]. Our collaborator Prof. Selaru and team at Johns Hopkins Medical School have established 37 primary patient-derived organoid (PDO) cultures from resected HCC tissues; and tested a library of Food and Drug Administration (FDA-approved cancer drugs across all 37 PDO cultures. They found that bortezomib (BTZ), a proteasome inhibitor that is approved for multiple myeloma and some forms of chronic myelogenous leukemia (CML) is highly effective across all tested PDO lines. Furthermore, BTZ has proven to be more effective than any of the currently approved FDA drugs for unresectable HCCs across all 37 PDO lines. However, BTZ under high dose systemic exposure has strong side effect that can lead to organ dysfunction and even lethality[3, 4]. This limitation hampers its potential clinical translation. Therefore, in order to improve the therapeutic efficiency of the drug, we aim to develop a strategy to decrease the systemic toxicity and expand the therapeutic window by developing a sustained release formulation of BTZ that can provide a local delivery of the drug in a controlled manner[5-8].

Currently, common strategies for the delivery of BTZ include the application of polymer, mesoporous silica, graphene oxide and liposomal nanoparticle systems[9-12]. However, few of them have focused on the construction of a local sustained release formulation of BTZ, therefore it is of great significance to develop an effective formulation that can be translated into clinical application in future use. There is a recent report using poly(lactic-co-glycolic acid) (PLGA) nanoparticle as carrier to achieve an extended release of BTZ. However, the complicated emulsion method employed has compromised the stability and reproducibility of the nanoparticle preparation and thus rendered it hard to reproduce[11]. Here, we report a new nanoparticle formulation prepared under facile process using our newly developed sequential Flash Nanocomplexation (FNC)/Flash Nanoprecipitation (FNP) technique. We explored the possibility of constructing a quaternary nanoparticle structure combining a ternary complex of tannic acid (TA), BTZ and ovalbumin (OVA) as core with coating of PEG-PLGA polymer matrix.

Tannic acid (TA) has been reported as a carrier in nanoparticulate protein release system, owing to its unique structure and ability to form hydrogen bonds with proteins[13, 14]. Similar to its binding with protein, the polyphenol structure of TA provides various bonding capacity towards BTZ including π-π stacking, hydrophobic interaction, and hydrogen bond, which makes it an ideal choice as a "BTZ cage" in the nanoparticle system[12, 15, 16]. The addition of OVA was expected to lower the highly negatively charged complex surface and increase the hydrophobicity thus helps with the PEG-PLGA coating. The sequential FNC/FNP platform can achieve a controlled nanoparticle assembly and release behavior by manipulating formulation parameters including mixing speed, pH, and concentrations, avoiding cumbersome operations typically used in the emulsion methods. This new method and new nanoparticle system hold great

clinical translation potential due to the obvious advantages in terms of particle size uniformity, high loading capacity, good control over release duration, reproducibility, and high scalability. We also studied the retention rate of BTZ-loaded nanoparticles and the tumor-killing effect in patient-derived xenograft (PDX) *via* intratumoral injection to test the potential therapeutic outcomes of local sustained delivery approach for BTZ.

Chapter 2

Experimental Approach and Methods

2.1 Devices and materials

Bortezomib was purchased from LC Laboratories (Woburn, MA, U.S.). Tannic acid (TA) and albumin from chicken egg white (ovalbumin) was purchased from Sigma-Aldrich (St. Louis, MO, U.S.). 5k-20k polyethylene glycol–poly(lactic acid-co-glycolic acid)(PEG-PLGA) was purchased from Poly SciTech®, Akina (West Lafayette, IN, U.S). Float-A-Lyzer® G2 dialysis device was purchased from Repligen (Waltham, MA, USA). Ultrafiltration tube was purchased from Sartorius (Göttingen, Germany). NE-4000 programmable multi-channel syringe pump was purchased from New Era Pump Systems, Inc (Farmingdale, NY, U.S.). 5 ml NORM-JET® syringe was purchased from VWR™ (Radnor, PA, U.S.). Thermo Scientific™ Hypersil™ BDS C18 HPLC Columns (4.6 mm×250 mm) was purchased from Thermo Fisher Scientific (Waltham, MA, U.S.). HPLC grade water, HPLC grade acetonitrile were purchased from Thermo Fisher Scientific (Waltham, MA, U.S.).

2.2 Preparation of BTZ-loaded nanoparticles

BTZ-loaded nanoparticles were prepared using a sequential FNC/FNP process (Figure. 1). The working solutions were prepared as follow: (1) BTZ was dissolved in a solvent composed of dimethyl sulfoxide (DMSO):distilled water (10:90, v/v) at a concentration of 1 mg/ml; (2) Tannic acid (TA) was dissolved in distilled water (pH = 5) at a

concentration of 4 mg/ml; (3) OVA was dissolved in distilled water (pH = 7.5) at a concentration of 1 mg/ml; and (4) PEG-PLGA was dissolved in pure acetonitrile at a concentration of 3, 5, or 7 mg/ml. Controlled by two digital syringe pumps, solutions of BTZ and TA were simultaneously injected into the two-inlet confined impingement jets (CIJ) mixer under a flow rate of 1, 3, 5 ml/min to form the BTZ-TA complex (Step 1, Figure 1). Then the BTZ/TA complex and OVA were simultaneously injected into the two-inlet CIJ mixer under a flow rate of 1, 8, 15 ml/min to coat the complex with a layer of OVA (Step 2). Finally, the BTZ/TA complex or OVA/BTZ-TA complex, water and PEG-PLGA were injected into a 3-inlet multi inlet vortex mixer for the FNP step under a flow rate of 3, 6, 10 ml/min (Step 3). The first 1 ml of the efflux mixture may contain less well-defined nanoparticles during the initial establishment of the steady flow, and therefore was discarded. The resulted nanoparticles were dialyzed in a 3.5-kDa dialysis tube for 4 hours to remove excess components and organic solvents before use.

2.3 Characterization

In order to find the optimal formulation based on out sequential FNC/FNP platform, the size uniformity and surface charge of BTZ-TA, BTZ-TA-OVA nanocomplex and BTZ-loaded nanoparticle were measured by the dynamic light scattering (DLS) analysis using Malvern Zetasizer Nano ZS at 25 ℃. To evaluate the encapsulation efficiency (EE) and loading level (LD), 5 ml of freshly prepared BTZ-loaded nanoparticle was dialyzed in DI water using 3.5 kDa dialysis bag for 4 hours and then lyophilized using a FreeZone Triad Benchtop Freeze Dryers (Labconco, USA) at 25 ℃ and 10 Pa for 36 hours. The dried nanoparticles were weighed and then dissolved in 5 ml acetonitrile and measured by HPLC using UV-vis spectroscopy at 280 nm to determine the remaining

(encapsulated) BTZ concentration. All measurements were performed in triplicates.

$$EE\ (\%)\ =\ \left(\frac{Amount\ of\ encapsulated\ BTZ}{Total\ amount\ of\ BTZ\ added}\right) \times 100\% \qquad (1)$$

$$LD\ (\%)\ =\ \left(\frac{Amount\ of\ encapsulated\ BTZ}{Total\ amount\ of\ lyophilized\ nanoparticles}\right) \times 100\% \qquad (2)$$

2.4 Storage stability

The storage stability of BTZ-loaded nanoparticles was evaluated both in the solution form and the lyophilized form. The colloidal stability was evaluated by storing BTZ-nanoparticle suspension in 4 ℃ for 30 days and measuring the change in size and surface charge. The lyophilization stability was evaluated by applying the same lyophilization protocol (with addition of 9.5% trehalose as cryoprotectant). The freeze-dried powder was stored at -80 ℃. After 30 days, the size and polydispersity index of the lyophilized nanoparticles were monitored upon reconstitution.

2.5 In vitro release of BTZ from nanoparticles

The *in vitro* release behaviors of BTZ-loaded nanoparticles were conducted using a dialysis method. Briefly, 1 ml of BTZ-loaded nanoparticle suspension was pipetted into a 100-kDa dialysis tube and incubated in 9 ml of PBS (10 mM, pH 7.4, with 0.1% tween 20) at 37 ℃ on a shaker at 100 rpm. At predominant time points (8, 16, 32, 56, 80, 104, 128 hours), 0.2 ml of the release medium was taken out and equivalent volume of fresh PBS was added. The concentration of released BTZ in the collected sample was measured using HPLC. The mobile phase composed of acetonitrile: water (60/40, v/v), maintaining a flow rate of 1 ml/min. The UV detector was set at 280 nm for absorption and fitting to a standard curve, then linked to computer software for data analysis.

2.6 MTT assay

Cells from three different patient-derived HCC organoids were separately seeded in a 96-well plate at a density of 1000 cells per well and allow to grow for 24 hours. Then, free BTZ (1, 0.1, 0.01 μM), NP-3 (1, 0.1, 0.01 μM) and same volume of PBS were added into each well and incubated for 4 and 8 days. After 4 incubation, medium was removed, and wells were washed with PBS. The MTT reagent was dissolved in medium to a final concentration of 0.5 mg/ml in each well, followed by incubation for 4 hours at 37°C. After removing the MTT-contained medium, DMSO solution (150 μL/well) was added, and the plate was shaken on a microplate stirrer for 10 minutes to dissolve the crystal. The OD value of each well was detected by a microplate reader (detection wavelength 570 nm).

2.7 *In vivo* retention at injection site using *Cy 7.5*-labelled nanoparticles

Cy 7.5 carboxylic acid was used to label PEG-PLGA as previously described[17]. Cy 7.5-labelled nanoparticles were prepared following the same formulation above with dye-labelled PEG-PLGA. The retention effect of nanoparticles was assessed using patient derived xenograft (PDX) model. Briefly, fresh human tumor tissue was harvested from HCC patients, then cut in small pieces ($2\times2\times2$ mm^3) and implanted subcutaneously in the right flank of NSG mice. Once tumors grew, a similar process (harvesting tumors from mice, mincing and inserting in new mice) was implemented. Mice at the 5th passage of PDX were utilized in this experiment. After implantation subcutaneously, the tumors were allowed to grow to approximately 1,000 mm^3. Five mice were subjected to intratumoral injection of 100 μL of Cy 7.5-labelled nanoparticles suspension, and the

biodistribution of Cy 7.5-nanoparticle was revealed by near infrared imaging using the IVIS system (PerkinElmer, US) with λ_{ex} 780 nm and λ_{em} 810 nm for 12 days post-administration. The retention rate of nanoparticles at injection site was calculated by comparing the remaining fluorescence intensity to the that of the original time point.

2.8 In vivo therapeutic effect of BTZ-loaded nanoparticles

The therapeutic effect of BTZ-loaded nanoparticles was assessed by monitoring the tumor-killing effect in PDX model mice following intratumoral injection. Briefly, mice were randomized to 3 groups with 5 mice in each group. Two treatment groups were administrated with 100 μL of free BTZ drug (0.5 mg/kg) twice a week, and 100 μL of BTZ-loaded nanoparticles (1 mg/kg) once a week, respectively. The control group was treated with 100 μL of PBS. The tumor size and body weight of the mice in different groups were measured two times per week throughout the 4-week period. The mice were euthanized after 4 weeks; and tumor tissues were collected to be analyzed.

Chapter 3

Experimental Results and Discussion

3.1 Formulation screening and characterization of the BTZ-loaded nanoparticles

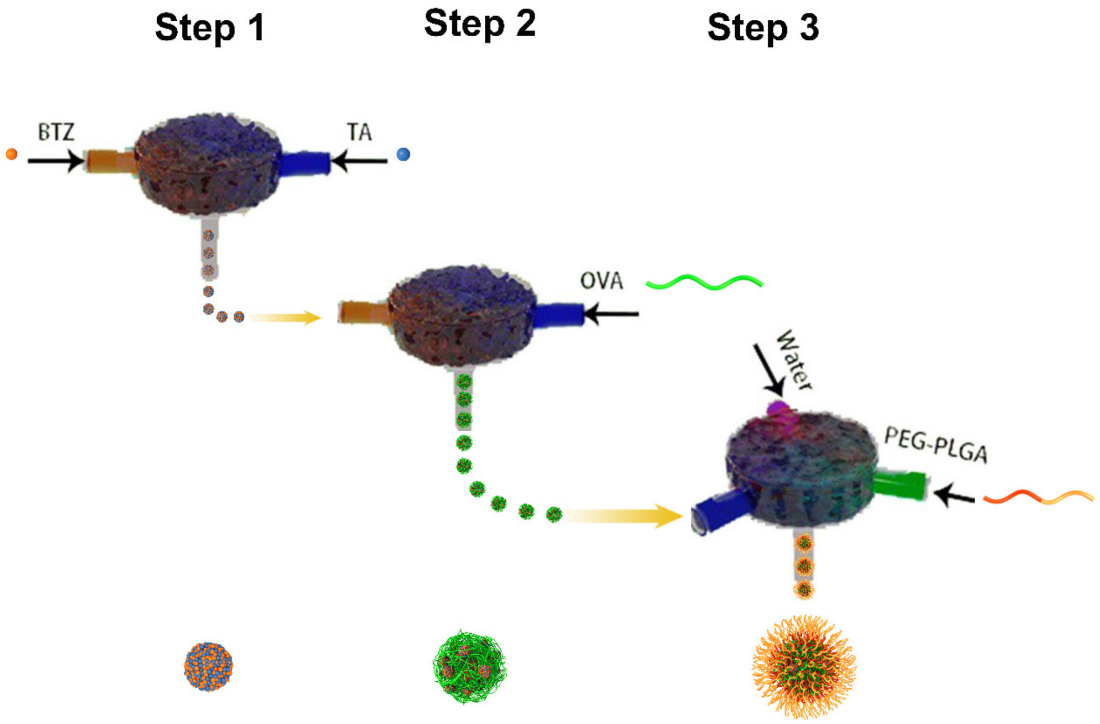

Figure 1. Schematic illustration of the sequential FNC /FNP method utilized in the BTZ-loaded nanoparticle preparation process.

The nanoparticle was assembled by a sequential FNC/FNP process as shown in Figure 1, in which the first step is to generate a TA-BTZ complex. We found that the uniformity of TA-BTZ complex is closely associated with flow rate as higher mixing rate will result in poorer size distribution (Figure 2A). We speculated that the complexation between TA and BTZ requires a certain reaction time, thus lower flowrate allowed the complexation process to happen within the mixing

chamber and render a uniform distribution of the BTZ-TA nanocomplex. Therefore, the flowrate of step one was set as 1 ml/min. Comparing to the flow rate to form TA-BTZ complex (1 ml/min), the formation of OVA-TA-BTZ complexes required a relatively high flow rate (15 ml/min) to ensure a uniform nanocomplex (Figure 2B), which necessitated the two-step FNC process instead of a one-step ternary mixing. As shown in Figure 2C, the final FNP step also requires a relatively high flow rate to render a uniform size distribution. Our interpretation is that the formation of OVA-TA-BTZ complex as well as the precipitation of polymer in the FNP step is relatively fast, therefore they need a higher mixing speed, which allows for a homogeneous distribution of all components within milliseconds for generating uniform nanoparticles instead of forming local aggregation due to inefficient mixing[18, 19].

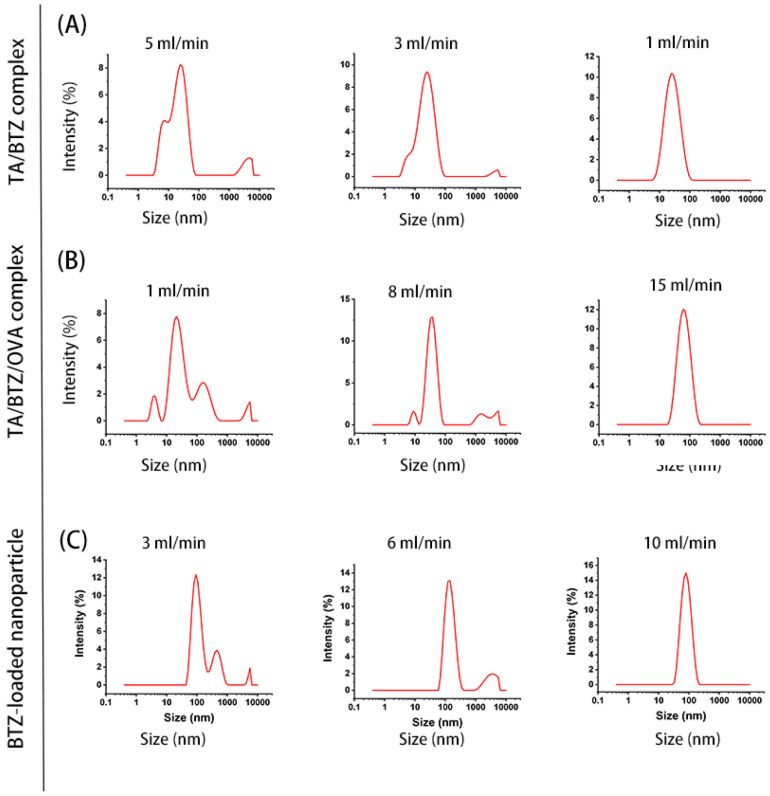

Figure 2. Formulation screening of the sequential FNC/FNP process. (A) Size distribution of TA-BTZ complex under different flow rate. (B) Size distribution of TA-BTZ-OVA complex under different flow rate. (C) Size distribution of BTZ-loaded nanoparticle under different flow rate.

The optimized BTZ-loaded nanoparticle showed a narrow size distribution (Figure 3A) and with

high encapsulation efficiency (~90%) and loading level (3% - 5%) of BTZ. We observed an increasing trend of particle size and surface charge with the addition of each component (Figure 3B), which indirectly suggests a construction of the BTZ-loaded nanoparticle in a stepwise assembly manner. The BTZ-TA nanocomplexes carried a high negative surface charge (-44.2 ± 0.3 mV), which is unfavorable for the coating of PEG-PLGA. By incorporating OVA into the complexes, the average surface charge was decreased to -20.8 mV. We expected that incorporation of OVA plays an essential role to enhance the compatibility between BTZ-TA complex and PEG-PLGA by decreasing surface charge and increasing hydrophobicity, thus enhanced the coating of outer polymeric matrix[20, 21]. The core-shell structure was the revealed by the TEM imaging shown in Figure 3C.

These nanoparticles also showed excellent colloidal stability in water for 30 days under 4 °C and preserved the same physical profile after reconstituting lyophilized samples that had been in storage at -20 °C for 1 months (Table 1).

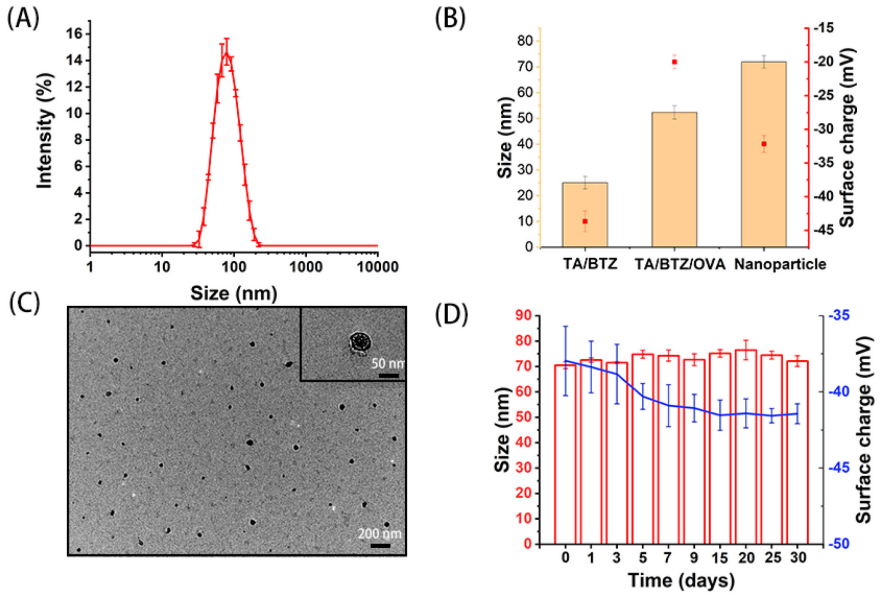

Figure. 3 Characterization of BTZ-loaded nanoparticles. (A) Size distribution of BTZ-loaded nanoparticles; (B) Surface charge and size change of nanoparticle along each step. (C) Transmission electron microscopy imaging of BTZ-loaded nanoparticles; (D) Colloidal stability as reflected by the average size of the BTZ-loaded

nanoparticles.

Table 1. Characteristics of freshly prepared *vs.* lyophilized-and-reconstituted BTZ-loaded nanoparticles.

Parameter	Freshly prepared	Reconstituted
Average size (nm)	72.3 ± 1.8	80.2 ± 2.4
Average zeta potential (mV)	-36.5 ± 0.8	-38.2 ± 0.5
Polydispersity index (PDI)	0.13 ± 0.01	0.15 ± 0.01
Rehydration time (sec)	-	< 15

All data are shown as means ± S.D. (n = 3).

3.2 In vitro release of BTZ-loaded nanoparticles

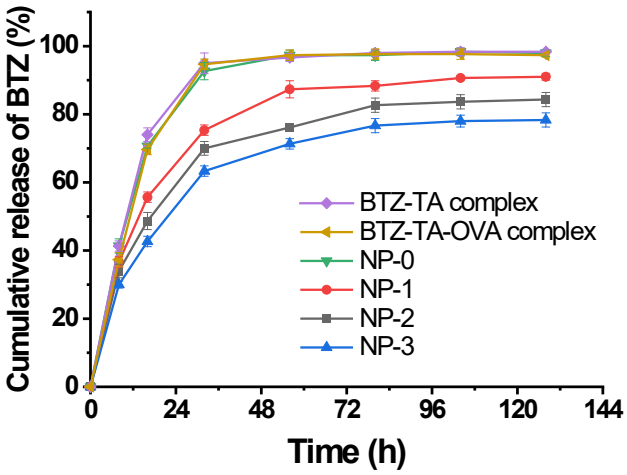

Figure 4. In vitro release study of different BTZ nano-formulations. BTZ-TA complex and BTZ-TA-OVA complex without PEG-PLGA coating; NP-0 refers to TA/BTZ complex coated directly with PEG-PLGA; NP-1, NP-2, NP-3 refer to BTZ/TA/OVA/PEG-PLGA nanoparticle prepared under different PEG-PLGA concentrations. The results are presented as mean ± S.D. (n = 3).

As shown in Figure 4, we compared the release behavior of different formulations in PBS (pH=7.4) under 37 ℃ for 128 hours. NP-0 refers to nanoparticles made by a two-step FNC/FNP method, in which BTZ-TA complex directly went through the FNP process without OVA complexation. NP-1, NP-2, NP-3 refer to BTZ-loaded

nanoparticles made by different concentration of PEG-PLGA (3, 5, 7, respectively). It is worth noting that NP-0 did not yield any measurable difference in release profile as compared with BTZ-TA and BTZ-TA-OVA nanocomplexes, suggesting a poor coating efficiency of PEG-PLGA onto the BTZ-TA complex surface. In contrast, NP-1, NP-2, NP-3 showed gradual extension of the release duration and lower release rate of BTZ from the nanoparticles. NP-3 achieved a release duration of around 5 days. These results are consistent with the hypothesis that BTZ-TA nanocomplexes carry too much surface charge to facilitate coating of the hydrophobic PLGA; and the incorporation of OVA effectively reduced the surface charge and polarity, thus increasing the rate of heterogenous nucleation of PEG-PLGA on the complex core[22, 23]. Furthermore, BTZ release rate can be reduced by increasing polymer concentration in the final coating process. This quaternary nanoparticle system endowed a high degree of flexibility in tuning release profile to satisfy various treatment options. This study provided the foundation for further optimization of the formulation to increase the duration of release.

3.3 In vitro efficacy of BTZ-loaded nanoparticles

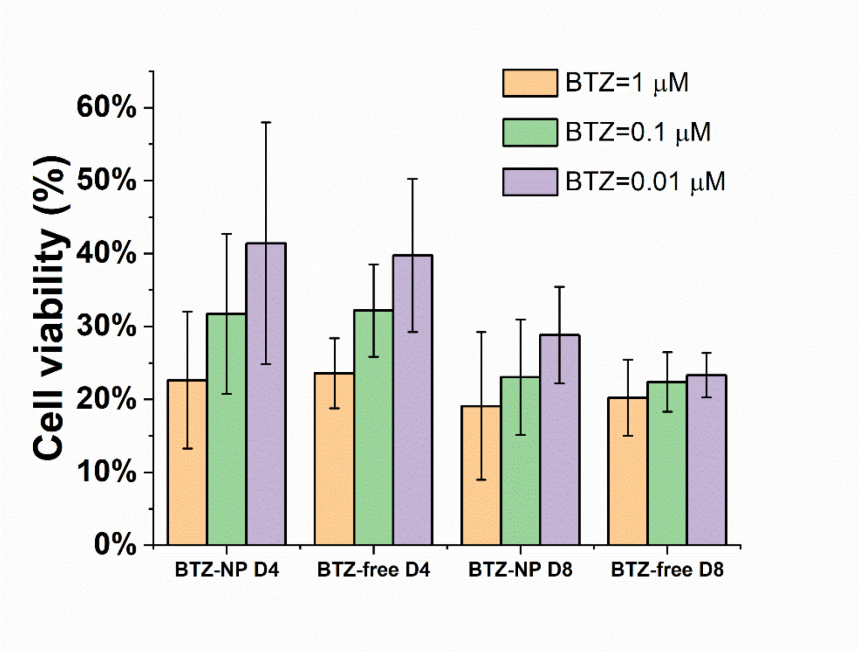

Figure 5. In vitro activity evaluation of BTZ-loaded nanoparticles. Cell viability results in different concentration of BTZ-loaded nanoparticles and free BTZ after 4 days or 8 days. The results are presented as mean ± S.D. (n = 3).

We first studied the *in vitro* bioactivity of BTZ-loaded nanoparticles by conducting MTT assay using different doses of BTZ. The tumor killing ability of BTZ-loaded nanoparticles was measured on three different patient derived cancer cells and compared with different formulations. As shown in Figure 5, there was no significant difference in cell viability between the cells treated with BTZ-loaded nanoparticles and free BTZ, indicating that the tumor-killing ability of BTZ-loaded nanoparticles was not compromised by the nano-formulating process and the sustained release manner. These results provide strong justification for *in vivo* testing to assess the long-acting tumor killing ability of the nanoparticles.

3.4 *In vivo* retention effect in tumor tissue following intratumoral injection of BTZ-loaded nanoparticles

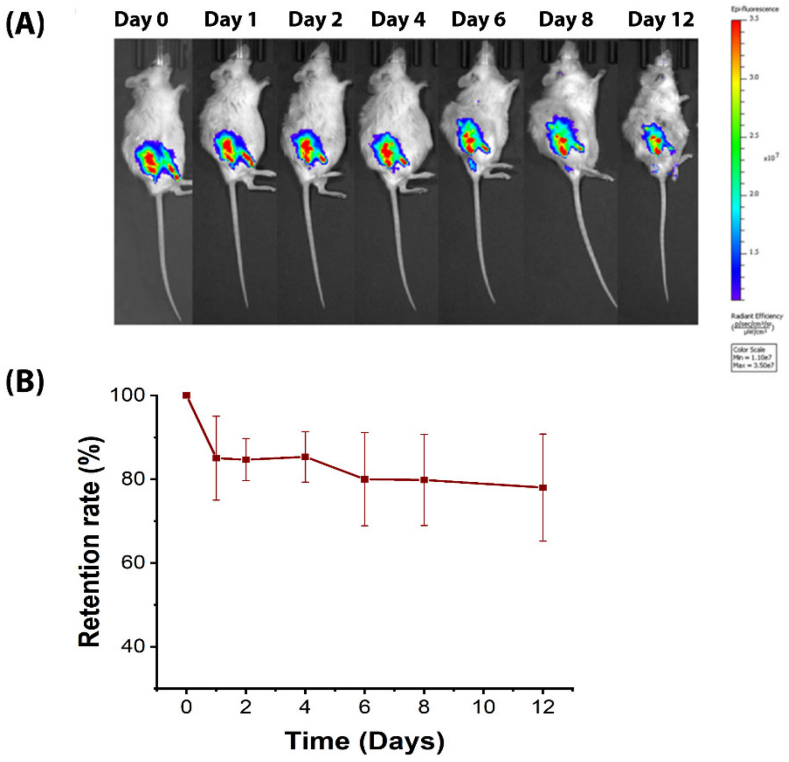

Figure 6. Biodistribution of the fluorescent dye-labeled nanoparticles after intra-tumoral injection. (A) In vivo fluorescence imaging of mice at different time points (0 – 12 d) after a single intratumoral injection of Cy 7.5-labelled nanoparticles. (B) Semi-quantification of fluorescence intensity of the Cy 7.5-labelled nanoparticle at injection site. The results are presented as mean ± S.D. (n = 5)

Our proposed aim to achieve a local sustained release using BTZ-loaded nanoparticles relies on that the nanoparticles will be sufficiently retained in the tumor tissue , rather than rapidly cleared into systemic circulation. Due to the enhanced permeability and retention (EPR) effect, nanosized agents tend to be enriched and retained in the tumor tissue[24-26]. In order to test our formulated BTZ for its ability to be retained in the tumor mass, we monitored the release of fluorescently dye-labeled nanoparticles after

intratumoral injection for 12 days. As shown in Figure 6A, the fluorescence intensity was maintained at a high level throughout the experiment, indicating an excellent retention of the nanoparticles in the tumor mass. This finding was further confirmed by the semi-quantitative analysis shown in Figure 6B, which ensured that the BTZ could be slowly released within the tumor tissue during the treatment period considering the retention time of more than 12 days is much longer than the release duration (~5 days).

3.5 In vivo tumor-inhibition effect of BTZ-loaded nanoparticles in patient-derived xenograft (PDX) model

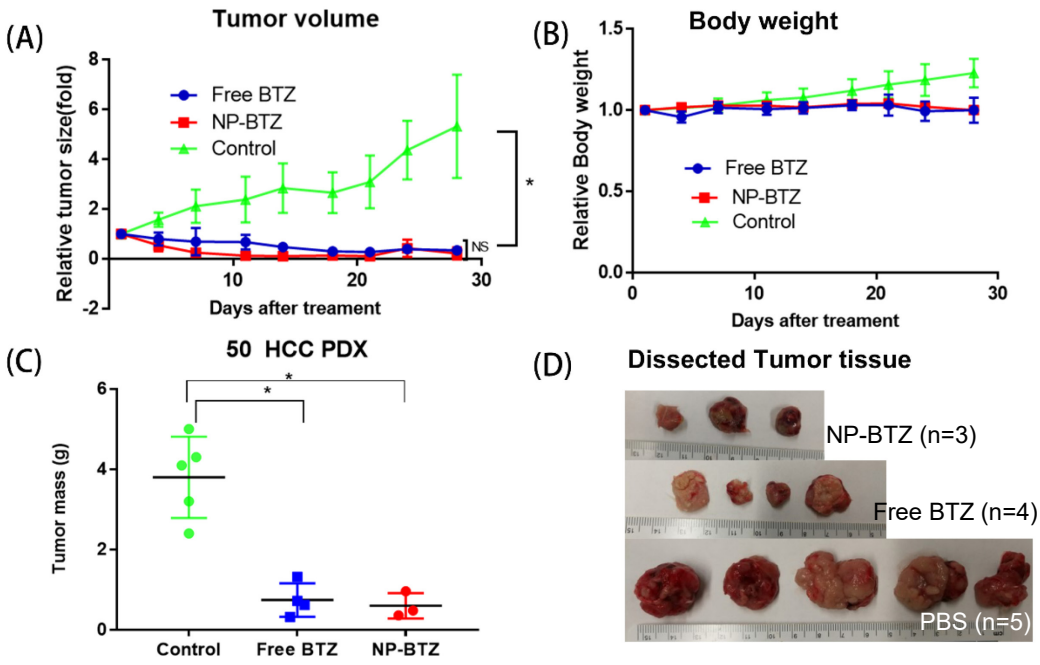

Figure 7. In vivo therapeutic outcomes of BTZ-loaded nanoparticles. (A) Relative tumor size as compared to original point in different treatment groups. (B) Relative body weight of mice as compared to original point in different groups. (C) Tumor weight measured at the end point of the treatment. (D) Gross pictures of the tumor tissues in each treatment groups.

The therapeutic effect of BTZ-loaded nanoparticles was assessed by measuring the

potency in inhibiting tumor growth following intratumoral injection (Figure 8). The dosages of free BTZ and BTZ-loaded nanoparticles were determined by a preliminary study assessing the tolerated dose of free BTZ to be 1 mg/kg, which killed mice within two days. In comparison, BTZ-loaded nanoparticles were tolerated well at the same dose. In this pilot study, we selected a dose of 0.5 mg/kg given twice weekly for free BTZ treatment, and doubled dose for BTZ-loaded nanoparticle treatment at a longer interval (1 mg of BTZ/kg, once per week). As shown in Figure 7A, the average tumor size in the control group increased by 5 folds over a 4-week period. Both the free BTZ and BTZ-loaded nanoparticle treatment successfully suppressed tumor growth completely. It appears that the BTZ-nanoparticles had a stronger tumor inhibiting effect at early time points (Days 6 to 14), considering that same total dose was given. Unfortunately, there are two mice in BTZ nanoparticle treatment group and one mouse in free BTZ group got pregnant near the end experiment. The tumor of pregnant mice started growing again even with treatments, therefore the data of which were removed from the results. There were no measurable differences in body weights of mice among all treatment groups throughout the entire treatment period (Figure 7B), except that the body weight of mice in the control group treated with PBS gradually increased after 2 weeks, presumably due to the overgrowth of tumor tissue. All mice were euthanized after 28 days and tumor tissue were collected to measure tumor mass directly (Figure 7C-D). The results (Figure 7C) matched the size measurement (Figure 7A) with a high level of consistence. Since all mice were originally implanted with similar size of tumor tissue, the dramatic difference between control group and treatment groups further demonstrated the significant tumor-killing ability of both BTZ formulations. More importantly, the BTZ-loaded nanoparticle treatment given at a lethal dose of BTZ (1 mg/kg), but did not yield any mortality, indicating the nano-formulated drug was

effective in lowering the systemic toxicity comparing to its free form as a result of a sustained release mechanism. Such a treatment option with a reduced systemic toxicity combining with high tumor-inhibition potency and less frequent administration, will greatly improve the therapeutic efficacy and patient compliance in clinical application.

Chapter 4

Conclusion and Outlook

We have developed a BTZ-loaded nanoparticle formulation that can achieve sustained release of BTZ using a new nanoencapsulation method that offers the advantages of continuous, tunable, and scalable manufacturing features. We established correlations between manufacturing parameters, nanoparticle characteristics, and drug release properties of the BTZ nanoparticles. By controlling the input parameters during manufacturing process, we are able to control the BTZ release behavior of nanoparticles. We have showed that this BTZ-loaded nanoparticle system could significantly lower the systemic toxicity, extend the retention of nanoparticles at the injection site to achieve local delivery, and show strong tumor inhibition effect with the same total dosage as the free drug, but given at a less dosing frequency. This new formulation can improve therapeutic efficacy and patient compliance.

Further improvement will focus on controlling the assembly kinetics and internal structure of the nanoparticles through gaining insight into the assembly mechanism and polymer coating kinetics, thus achieving higher BTZ loading level and tighter control of BTZ release profile. A well-defined nanoparticle structure will help us explore the full potential of the formulation. Beyond intratumor delivery, we plan to investigate the effectiveness of systemically administrated nanoparticles (such as intravenous injection) on delivery efficiency to the tumor that have multiple nodules in the liver (i.e. metastasis in the liver and other organs.

Chapter 5

References Cited

[1] F.X. Bosch, J. Ribes, J. Borràs, Epidemiology of Primary Liver Cancer, Seminars in liver disease 19(03) (1999) 271-285.

[2] J.M. Llovet, J. Zucman-Rossi, E. Pikarsky, B. Sangro, M. Schwartz, M. Sherman, G. Gores, Hepatocellular carcinoma, Nature Reviews Disease Primers 2(1) (2016) 16018.

[3] G. Zuccari, A. Milelli, F. Pastorino, M. Loi, A. Petretto, A. Parise, C. Marchetti, A. Minarini, M. Cilli, L. Emionite, D. Di Paolo, C. Brignole, F. Piaggio, P. Perri, V. Tumiatti, V. Pistoia, G. Pagnan, M. Ponzoni, Tumor vascular targeted liposomal-bortezomib minimizes side effects and increases therapeutic activity in human neuroblastoma, Journal of Controlled Release 211 (2015) 44-52.

[4] A. Hacihanefioglu, P. Tarkun, E. Gonullu, Acute severe cardiac failure in a myeloma patient due to proteasome inhibitor bortezomib, International Journal of Hematology 88(2) (2008) 219-222.

[5] Z. Lin, W. Gao, H. Hu, K. Ma, B. He, W. Dai, X. Wang, J. Wang, X. Zhang, Q. Zhang, Novel thermo-sensitive hydrogel system with paclitaxel nanocrystals: High drug-loading, sustained drug release and extended local retention guaranteeing better efficacy and lower toxicity, Journal of Controlled Release 174 (2014) 161-170.

[6] Y. Mao, X. Li, G. Chen, S. Wang, Thermosensitive Hydrogel System With Paclitaxel Liposomes Used in Localized Drug Delivery System for In Situ Treatment of Tumor: Better Antitumor Efficacy and Lower Toxicity, Journal of Pharmaceutical Sciences 105(1) (2016) 194-204.

[7] D.R. Kalaria, G. Sharma, V. Beniwal, M.N.V. Ravi Kumar, Design of Biodegradable Nanoparticles for Oral Delivery of Doxorubicin: In vivo Pharmacokinetics and Toxicity Studies in Rats, Pharmaceutical research 26(3) (2009) 492-501.

[8] L. Liang, S.-W. Lin, W. Dai, J.-K. Lu, T.-Y. Yang, Y. Xiang, Y. Zhang, R.-T. Li, Q. Zhang, Novel cathepsin B-sensitive paclitaxel conjugate: Higher water

solubility, better efficacy and lower toxicity, Journal of Controlled Release 160(3) (2012) 618-629.

[9] J.D. Ashley, J.F. Stefanick, V.A. Schroeder, M.A. Suckow, T. Kiziltepe, B. Bilgicer, Liposomal bortezomib nanoparticles via boronic ester prodrug formulation for improved therapeutic efficacy in vivo, J Med Chem 57(12) (2014) 5282-92.

[10] J. Shen, G. Song, M. An, X. Li, N. Wu, K. Ruan, J. Hu, R. Hu, The use of hollow mesoporous silica nanospheres to encapsulate bortezomib and improve efficacy for non-small cell lung cancer therapy, Biomaterials 35(1) (2014) 316-326.

[11] S. Shen, X.-J. Du, J. Liu, R. Sun, Y.-H. Zhu, J. Wang, Delivery of bortezomib with nanoparticles for basal-like triple-negative breast cancer therapy, Journal of Controlled Release 208 (2015) 14-24.

[12] Y. Hu, L. He, W. Ma, L. Chen, Reduced graphene oxide-based bortezomib delivery system for photothermal chemotherapy with enhanced therapeutic efficacy, Polymer International 67(12) (2018) 1648-1654.

[13] Z. He, Y. Hu, Z. Gui, Y. Zhou, T. Nie, J. Zhu, Z. Liu, K. Chen, L. Liu, K.W. Leong, P. Cao, Y. Chen, H.Q. Mao, Sustained release of exendin-4 from tannic acid/Fe (III) nanoparticles prolongs blood glycemic control in a mouse model of type II diabetes, Journal of controlled release : official journal of the Controlled Release Society 301 (2019) 119-128.

[14] Z. He, T. Nie, Y. Hu, Y. Zhou, J. Zhu, Z. Liu, L. Liu, K.W. Leong, Y. Chen, H.-Q. Mao, A polyphenol-metal nanoparticle platform for tunable release of liraglutide to improve blood glycemic control and reduce cardiovascular complications in a mouse model of type II diabetes, Journal of Controlled Release 318 (2020) 86-97.

[15] Z. Le, Y. Chen, H. Han, H. Tian, P. Zhao, C. Yang, Z. He, L. Liu, K.W. Leong, H.-Q. Mao, Z. Liu, Y. Chen, Hydrogen-Bonded Tannic Acid-Based Anticancer Nanoparticle for Enhancement of Oral Chemotherapy, ACS Applied Materials & Interfaces 10(49) (2018) 42186-42197.

[16] Y.-N. Jin, H.-C. Yang, H. Huang, Z.-K. Xu, Underwater superoleophobic coatings fabricated from tannic acid-decorated carbon nanotubes, RSC Advances 5(21) (2015) 16112-16115.

[17] G.P. Howard, G. Verma, X. Ke, W.M. Thayer, T. Hamerly, V.K. Baxter, J.E. Lee, R.R. Dinglasan, H.-Q. Mao, Critical size limit of biodegradable

nanoparticles for enhanced lymph node trafficking and paracortex penetration, Nano Research 12(4) (2019) 837-844.

[18] Y. Hu, Z. He, Y. Hao, L. Gong, M. Pang, G.P. Howard, H.-H. Ahn, M. Brummet, K. Chen, H.-w. Liu, X. Ke, J. Zhu, C.F. Anderson, H. Cui, C.G. Ullman, C.A. Carrington, M.G. Pomper, J.-H. Seo, R. Mittal, I. Minn, H.-Q. Mao, Kinetic Control in Assembly of Plasmid DNA/Polycation Complex Nanoparticles, ACS Nano 13(9) (2019) 10161-10178.

[19] Z. He, Y. Hu, T. Nie, H. Tang, J. Zhu, K. Chen, L. Liu, K.W. Leong, Y. Chen, H.Q. Mao, Size-controlled lipid nanoparticle production using turbulent mixing to enhance oral DNA delivery, Acta Biomater 81 (2018) 195-207.

[20] K.M. Pustulka, A.R. Wohl, H.S. Lee, A.R. Michel, J. Han, T.R. Hoye, A.V. McCormick, J. Panyam, C.W. Macosko, Flash Nanoprecipitation: Particle Structure and Stability, Molecular Pharmaceutics 10(11) (2013) 4367-4377.

[21] C. Wischke, S.P. Schwendeman, Principles of encapsulating hydrophobic drugs in PLA/PLGA microparticles, International Journal of Pharmaceutics 364(2) (2008) 298-327.

[22] W.S. Saad, R.K. Prud'homme, Principles of nanoparticle formation by flash nanoprecipitation, Nano Today 11(2) (2016) 212-227.

[23] C.J. Martínez Rivas, M. Tarhini, W. Badri, K. Miladi, H. Greige-Gerges, Q.A. Nazari, S.A. Galindo Rodríguez, R.Á. Román, H. Fessi, A. Elaissari, Nanoprecipitation process: From encapsulation to drug delivery, International Journal of Pharmaceutics 532(1) (2017) 66-81.

[24] Y. Nakamura, A. Mochida, P.L. Choyke, H. Kobayashi, Nanodrug Delivery: Is the Enhanced Permeability and Retention Effect Sufficient for Curing Cancer?, Bioconjugate chemistry 27(10) (2016) 2225-2238.

[25] R. Kinoshita, Y. Ishima, V.T.G. Chuang, H. Nakamura, J. Fang, H. Watanabe, T. Shimizu, K. Okuhira, T. Ishida, H. Maeda, M. Otagiri, T. Maruyama, Improved anticancer effects of albumin-bound paclitaxel nanoparticle via augmentation of EPR effect and albumin-protein interactions using S-nitrosated human serum albumin dimer, Biomaterials 140 (2017) 162-169.

[26] D. Kalyane, N. Raval, R. Maheshwari, V. Tambe, K. Kalia, R.K. Tekade, Employment of enhanced permeability and retention effect (EPR): Nanoparticle-based precision tools for targeting of therapeutic and diagnostic agent in cancer, Materials Science and Engineering: C 98 (2019) 1252-1276.